Photon radiation in $e^+e^- \to$ hadrons at low energies with `carlomat_3.1`

Fred Jegerlehner
fjeger@physik.hu-berlin.de
Work done by Karol Kołodziej
Eur.Phys.J. C77 (2017) no.4, 254

RMC WG meeting Mainz, 30 June 2017

Outline of Talk:

- Effective field theory: the Resonance Lagrangian Approach, broken HLS
- A minimal version: VMD + sQED solving the τ vs e^+e^- puzzle
- Global fit of BHLS parameters and prediction of $F_\pi(s)$
- SM prediction of a_μ using BHLS predictions for $a_\mu^{\rm LO,had}$
- Lessons and Outlook

Introduction

Study of photon radiation at tree level incl. some form factors for low energy hadron production in e^+e^-–annihilation

F. Jegerlehner and K. Kołodziej, Eur. Phys. J. C **77** (2017) no.4, 254 doi:10.1140/epjc/s10052-017-4816-7 [arXiv:1701.01837 [hep-ph]].

- K. Kołodziej, carlomat_3.1 *version of the program dedicated to the description of processes of electron-positron annihilation to hadrons at low centre of mass energies*, http://kk.us.edu.pl/carlomat.html.

- K. Kołodziej, Comput. Phys. Commun. 180 (2009), 1671. arXiv:0903.3334[hep-ph] http://dx.doi.org/10.1016/j.cpc.2009.03.011

❏ Implements HLS Feymanrules with couplings from global HLS fit, combined with sQED for photon radiation of pions.

❏ Some features complementary to generator like PHOKHARA, I think.

Hiddel Local Symmetry Feynman Rules

HLS Lagrangian and global fit couplings see:

```
M. Benayoun, P. David, L. DelBuono and F. Jegerlehner,
``An Update of the HLS Estimate of the Muon g-2,''
Eur.\ Phys.\ J.\ C {\bf 73} (2013) 2453
doi:10.1140/epjc/s10052-013-2453-3
[arXiv:1210.7184 hep-ph]].}
```

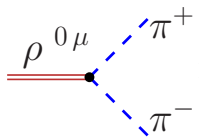

$$:= \; -\mathrm{i}\, g_{\rho\pi\pi}\,(p_- - p_+)^\mu$$

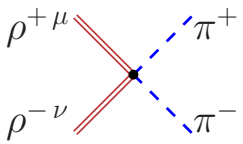

$$:= \; 2\,\mathrm{i}\, g^2_{\rho\pi\pi}\, g^{\mu\nu}$$

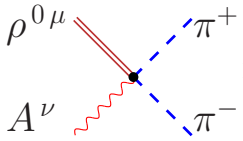

$$:= \; 2\,\mathrm{i}\, e\, g_{\rho\pi\pi}\, g^{\mu\nu}$$

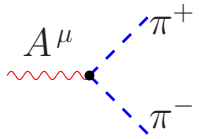

$$:= \; -\mathrm{i}\, e\,(p_- - p_+)^\mu$$

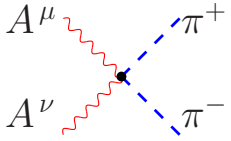

$$:= \; 2\,\mathrm{i}\, e^2\, g^{\mu\nu}$$

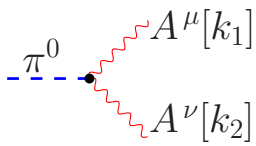

$$:= \; e^2\, g_{\pi\gamma\gamma}\, \varepsilon^{\mu\nu\alpha\beta}\, k_{1\alpha} k_{2\beta}$$

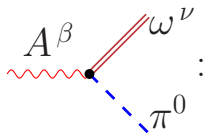

$$:= \; -\mathrm{i}\, e\, g_{\omega\gamma\pi}\, \varepsilon^{\mu\nu\alpha\beta}\, p_{\gamma\alpha} p_{\omega\mu}$$

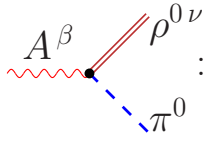

$$:= \; -\mathrm{i}\, e\, g_{\rho^0\gamma\pi^0}\, \varepsilon^{\mu\nu\alpha\beta}\, p_{\gamma\alpha} p_{\rho\mu}$$

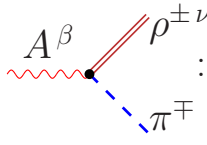

$$:= \; -\mathrm{i}\, e\, g_{\rho^{\pm}\gamma\pi^{\mp}}\, \varepsilon^{\mu\nu\alpha\beta}\, p_{\gamma\alpha} p_{\rho\mu}$$

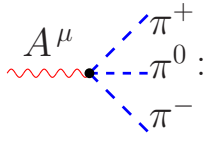

$$:= \; -e\, g_{\gamma\pi\pi\pi}\, \varepsilon^{\mu\nu\alpha\beta}\, p_{0\nu} p_{+\alpha} p_{-\beta}$$

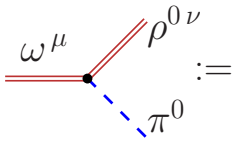

$$:= \; g_{\omega\rho\pi}\,\varepsilon^{\mu\nu\alpha\beta}\,p_{\omega\alpha}p_{\rho\beta}$$

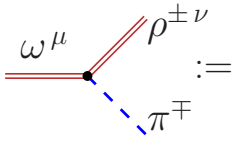

$$:= \; g_{\omega\rho\pi}\,\varepsilon^{\mu\nu\alpha\beta}\,p_{\omega\alpha}p_{\rho\beta}$$

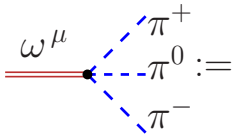

$$:= \; -\,g_{\omega\pi\pi\pi}\,\varepsilon^{\mu\nu\alpha\beta}\,p_{0\nu}p_{+\alpha}p_{-\beta}$$

$$g_{\rho\pi\pi} = 6.505(3)$$
$$g_{\omega\pi\pi} = 0.408(61)$$
$$g_{\pi\gamma\gamma} = -\frac{N_c}{24\pi^2 F_\pi}\,(1 - c_4)$$
$$g_{\gamma\pi\pi\pi} = -\frac{N_c}{12\pi^2 F_\pi^3}\,\left[1 - \frac{3}{4}\,(c_1 - c_2 + c_4)\right]$$
$$g_{\omega\pi\pi\pi} = -\frac{3N_c g}{16\pi^2 F_\pi^3}\,(c_1 - c_2 - c_3)$$
$$g_{\rho^\pm\pi^\mp\gamma} = \frac{G}{2}$$
$$g_{\rho^0\pi^0\gamma} = \frac{G}{2}$$
$$g_{\omega\pi^0\gamma} = \frac{3G}{2}$$
$$G = -\frac{g}{4\,\pi^2\,f_\pi}\,\frac{c_3 + c_4}{2}$$

$g_{\omega\rho\pi} = \frac{C}{2}$,
$C = -\frac{N_C\, g^2}{4\,\pi^2\, f_\pi}\, c_3$,
$N_c = 3$,
$F_\pi = 92.42$ MeV,
$g \equiv g_{\rm HLS} = 5.578(1)$,
$c_4 \approx c_3$, $(c_3 + c_4)/2 \approx c_3 = 0.920(4)$,
$c_1 - c_2 = 1.226(26)$,
$f_{\rho\gamma} = 2\, g_{\rho\gamma\gamma}\, f_\pi^2$,
$f_{\omega\gamma} = \frac{1}{3}\, f_{\rho\gamma}$

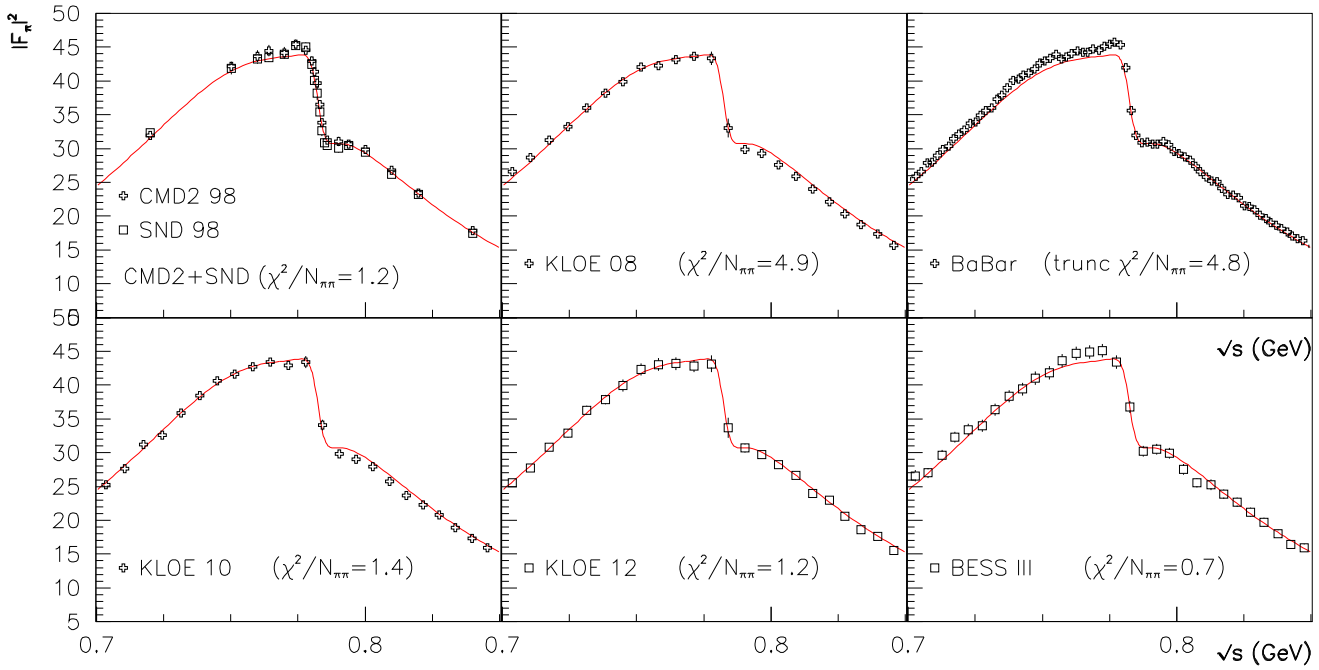

Comparing the τ+PDG prediction (red curve) of the pion form factor in e^+e^- annihilation in the $\rho-\omega$ interference region

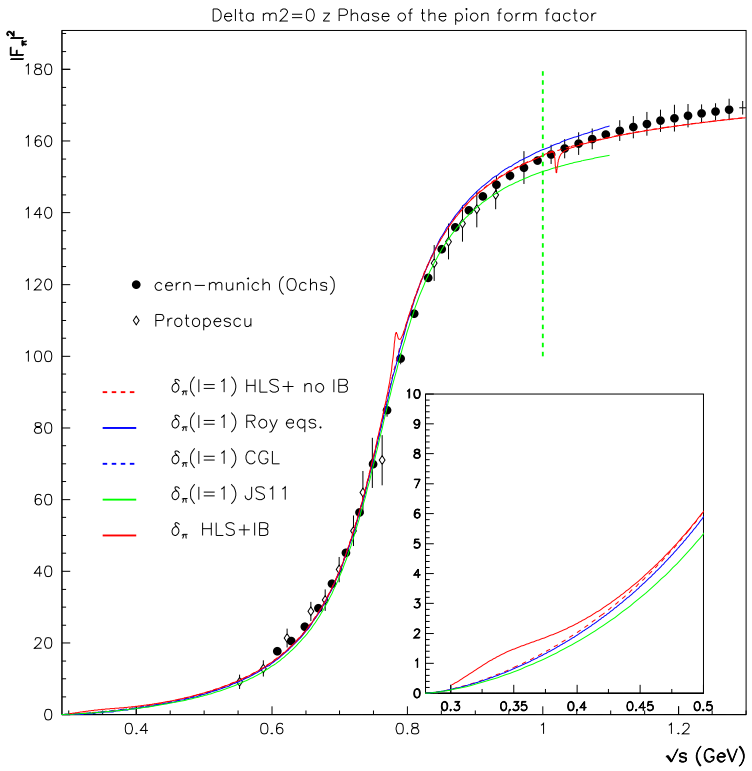

The HLS model at work. The left panel shows the global HLS model fit of the $\pi\pi$ channel together with the data from Novosibirsk, Frascati and Beijing. The right panel shows the P–wave $\pi^+\pi^-$ phase–shift data and predictions from Leutwyler, Colangelo and F.J.-Szafron together with the broken HLS phase–shift

sQED:

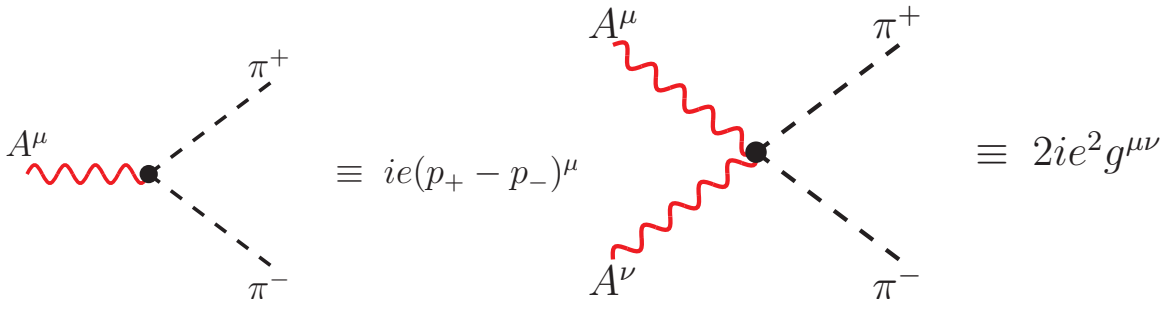

Is sQED model viable?

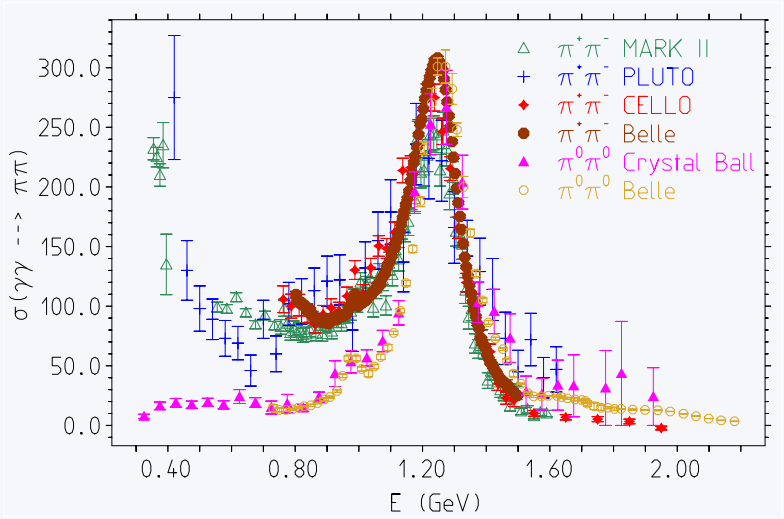

How photons couple to pions? This is obviously probed in reactions like $\gamma\gamma \to \pi^+\pi^-, \pi^0\pi^0$. Data infer that below about 1 GeV photons couple to pions as point-like objects (i.e. to the charged ones overwhelmingly), at higher energies the photons see the quarks exclusively and form the prominent tensor resonance $f_2(1270)$. The $\pi^0\pi^0$ cross section in this figure is enhanced by the isospin symmetry factor 2, by which it is reduced in reality.

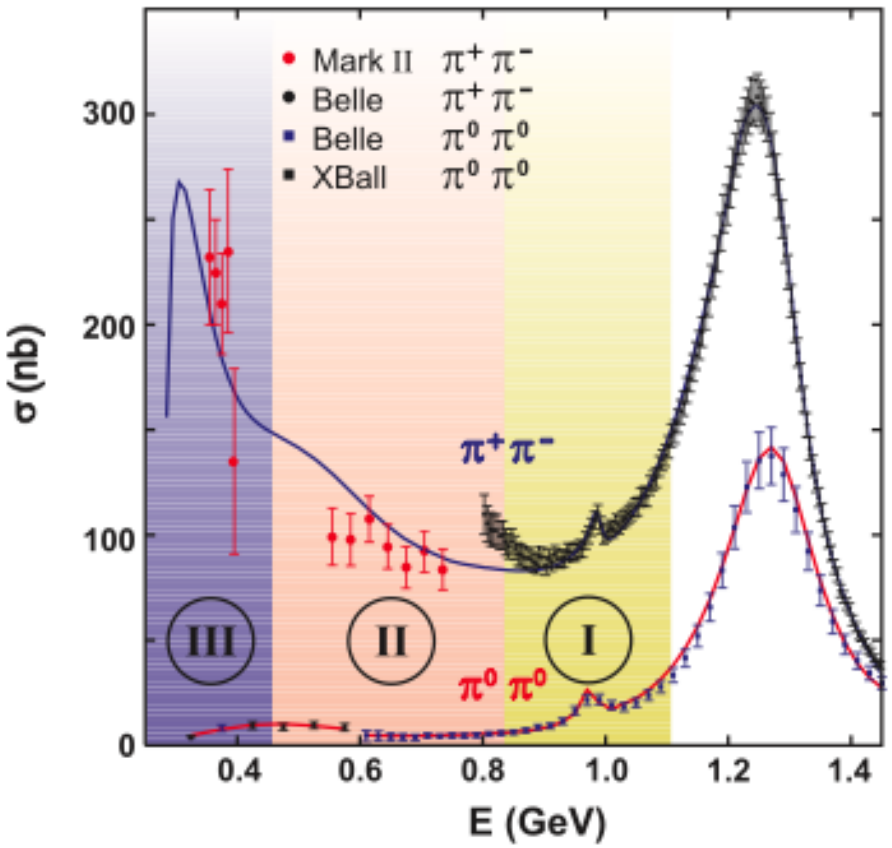

Normalization as in reality: $\sigma(\pi^0\pi^0)/\sigma(\pi^+\pi^-) = \frac{1}{2}$ at the $f_2(1270)$ peak
(art work by Mike Pennington)

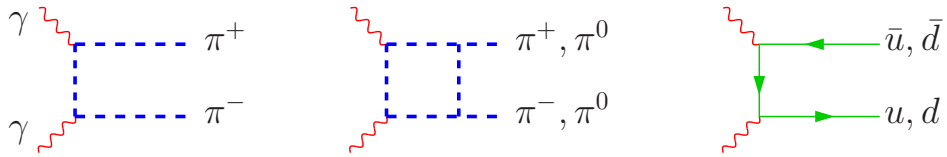

Di-pion production in $\gamma\gamma$ fusion. At low energy we have direct $\pi^+\pi^-$ production and by strong rescattering $\pi^+\pi^- \to \pi^0\pi^0$, however with very much suppressed rate. Above about 1 GeV, resolved $q\bar{q}$ couplings seen.

Strong tensor meson resonance in $\pi\pi$ channel $f_2(1270)$ with photons directly probe the quarks!

Pion Form Factor Implemented

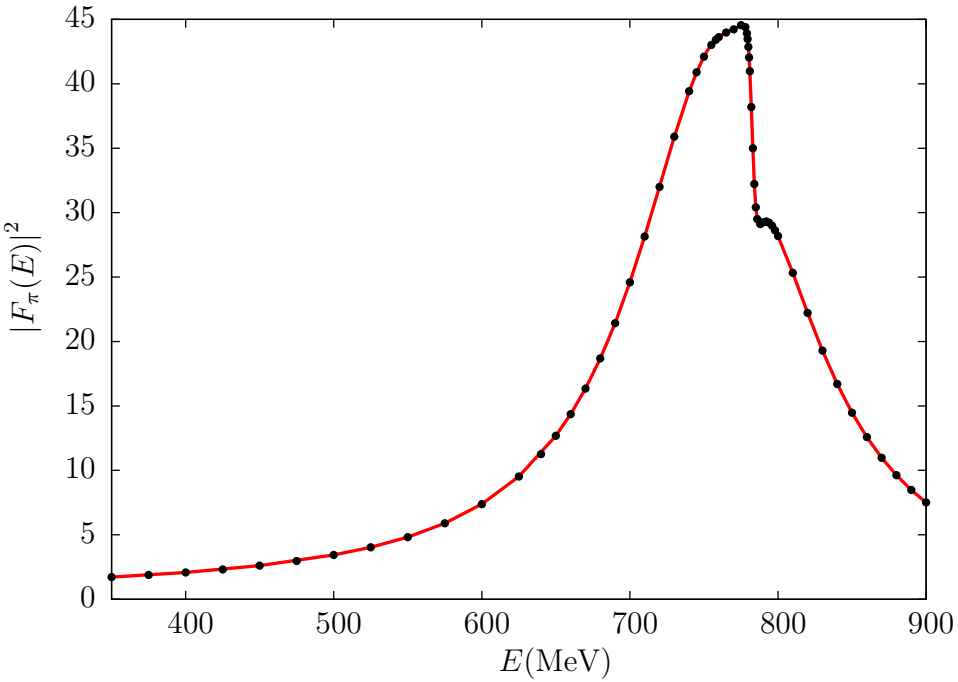

The EM charged pion form factor calculated by direct calls to the subroutine for $F_\pi(s)$ (points) and with the MC program generated automatically (solid line).

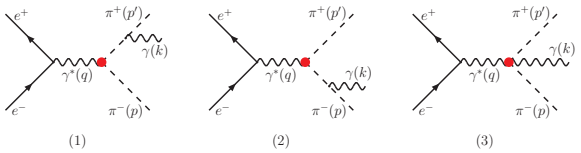

FSR Feynman diagrams of process $e^+e^- \to \pi^+\pi^-\gamma$ in the LO. The relevant four momenta are indicated in parentheses and blobs represent the charged pion form factor.

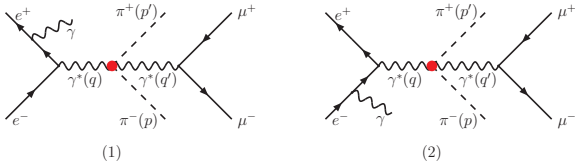

ISR Feynman diagrams of process $e^+e^- \to \pi^+\pi^-\gamma$ in which the choice of four momentum transfer in the charged pion form factor, represented by the red blob, may be ambiguous.

Non-SM Vertices Implemented

$\equiv -ef_{AV}(q^2)\, g^{\mu\nu}, \qquad V = \rho^0, \omega, \phi, \rho_1, \rho_2$

The $\gamma - V$-mixing terms considered in the present work; ρ_1 and ρ_2 stand for $\rho(1450)$ and $\rho(1700)$, respectively.

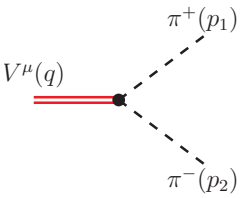

$\equiv if_{V\pi^+\pi^-}(q^2)(p_1 - p_2)^\mu,$
$V = \rho^0, \omega, \phi, \rho_1, \rho_2$

(a)

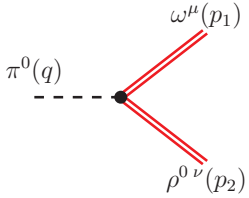

$\equiv f_{\pi^0\omega\rho^0}(q^2)\varepsilon^{\mu\nu\alpha\beta}p_{1\,\alpha}p_{2\,\beta}$

(b)

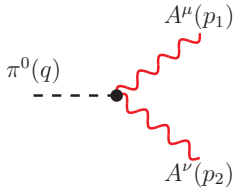

$\equiv e^2 f_{\pi^0 AA}(q^2)\varepsilon^{\mu\nu\alpha\beta}p_{1\,\alpha}p_{2\,\beta}$

(c)

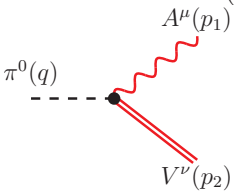

$\equiv ief_{\pi^0 AV}(q^2)\varepsilon^{\mu\nu\alpha\beta}p_{1\,\alpha}p_{2\,\beta}$
$V = \rho^0, \omega$

(d)

Triple vertices of the HLS relevant for the present work.

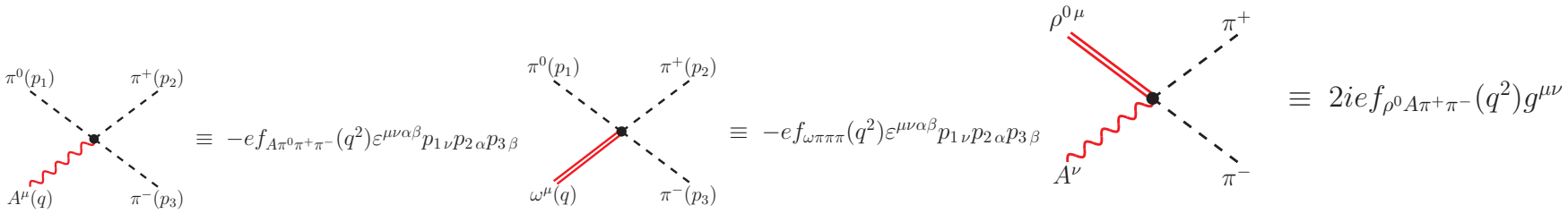

(a) (b) (c)

Quartic vertices of the HLS model taken into account in the present work.

Results

Process	ISR			full LO		
$e^+e^- \to$	# diags	σ	$\sigma\|_{\varepsilon(k)=k}$	# diags	σ	$\sigma\|_{\varepsilon(k)=k}$
$\pi^+\pi^-\gamma$	2	2.041(4)e+4	1.04(1)e–28	5	2.249(4)e+4	2.73(2)e–28
$\pi^+\pi^-\pi^0\gamma$	32	409(1)	2.21(3)e–30	156	481.5(6)	3.011(1)e–2
$\pi^+\pi^-\mu^+\mu^-\gamma$	26	4.344(9)e–2	4.62(5)e–34	107	6.449(8)e–2	6.42(5)e–34
$\pi^+\pi^-\pi^+\pi^-\gamma$	36	2.029(5)e–3	2.14(3)e–35	200	3.320(5)e–3	3.03(2)e–35
$\pi^+\pi^-\gamma\gamma$	6	1.445(14)e+3	1.22(4)e–29	44	2.131(8)e+3	2.08(3)e–29
$\pi^+\pi^-\mu^+\mu^-\gamma\gamma$	90	1.127(7)e–3	1.16(4)e–35	1272	2.535(8)e–3	9.56(1)e–19
$\pi^+\pi^-\pi^+\pi^-\gamma\gamma$	120	4.68(3)e–5	4.6(1)e–37	2772	1.303(4)e–4	4.969(4)e–15

The cross sections in pb at $\sqrt{s} = 1$ GeV and the corresponding $U(1)$ gauge invariance tests. The numbers in parentheses show the MC uncertainty of the last decimals.

The differential cross sections of process at $\sqrt{s} = 0.8$ GeV, $\sqrt{s} = 1$ GeV and $\sqrt{s} = 1.5$ GeV:

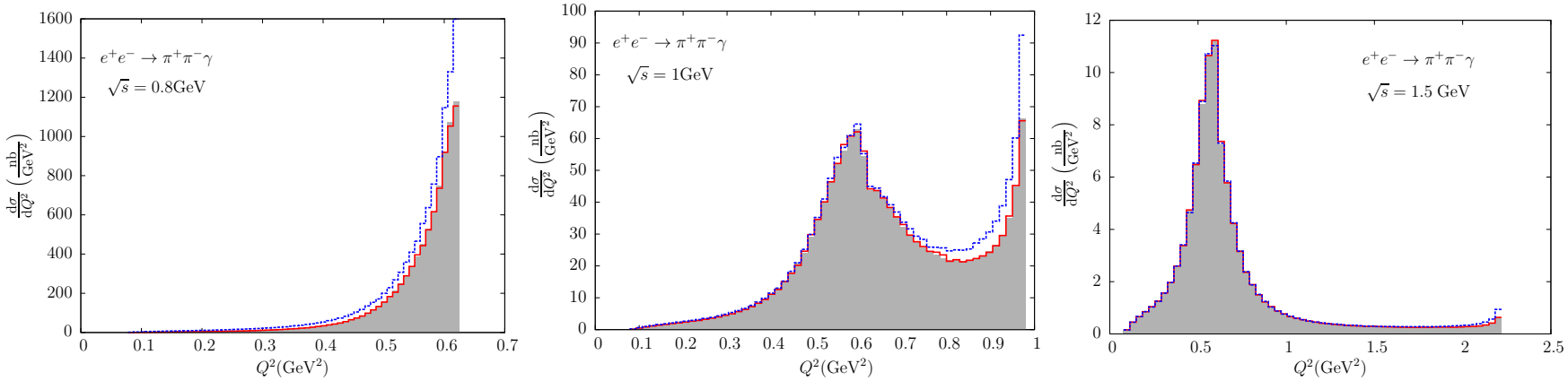

The differential cross sections of process $e^+e^- \to \pi^+\pi^-\gamma$ as functions of invariant mass of the $\pi^+\pi^-$-pair. The solid line and the shaded histogram represent the ISR cross section, obtained with the MC program and with the known analytic formula, respectively, and the dashed line represents the full LO result. The difference between solid and dashed lines represents the FSR correction.

LO $e^+e^- \to \pi^+\pi^-\gamma$ with external $F_\pi(s)$ vs. HLS model with fixed couplings exhibiting 26 Feynman diagrams.

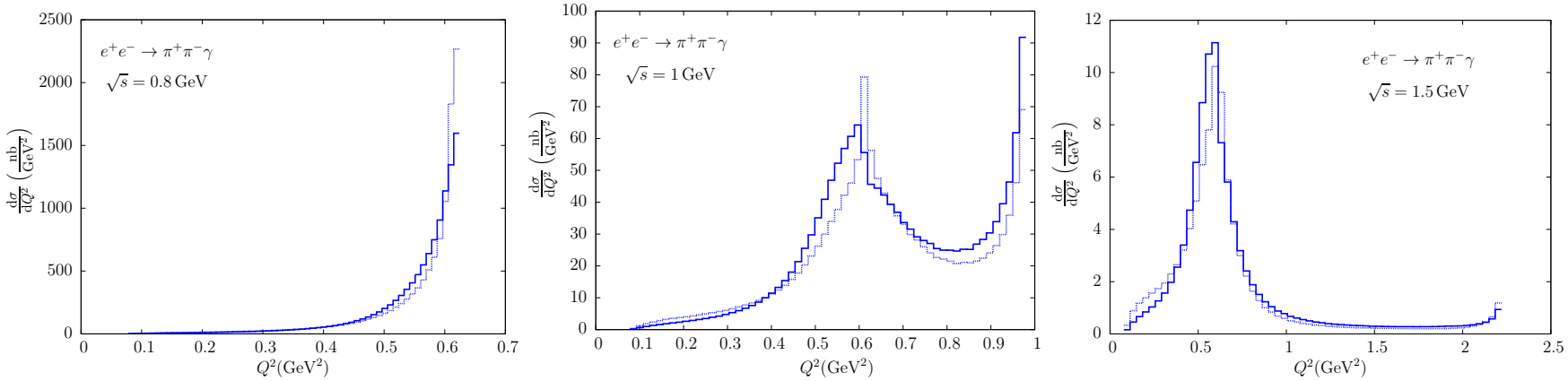

The differential cross sections of $e^+e^- \to \pi^+\pi^-\gamma$ as functions of invariant mass of the $\pi^+\pi^-$-pair computed in a model with the charged pion form factor (solid lines) and in the HLS model with fixed couplings (dotted lines).

The differential cross sections of processes $e^+e^- \to \pi^+\pi^-\pi^0\gamma$, $e^+e^- \to \pi^+\pi^-\mu^+\mu^-\gamma$ and $e^+e^- \to \pi^+\pi^-\pi^+\pi^-\gamma$ corresponding to those plotted next as functions of the invariant mass of the $\pi^+\pi^-\pi^0$-, $\pi^+\pi^-\mu^+\mu^-$-, or $\pi^+\pi^-\pi^+\pi^-$-system.

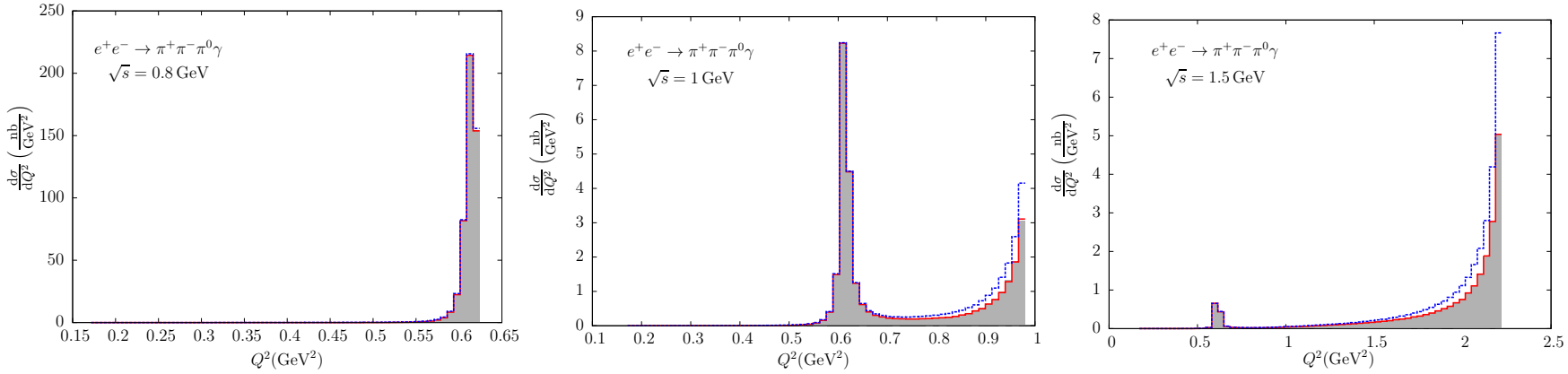

The differential cross sections of $e^+e^- \to \pi^+\pi^-\pi^0\gamma$ as functions of invariant mass of the $\pi^+\pi^-\pi^0$-system.

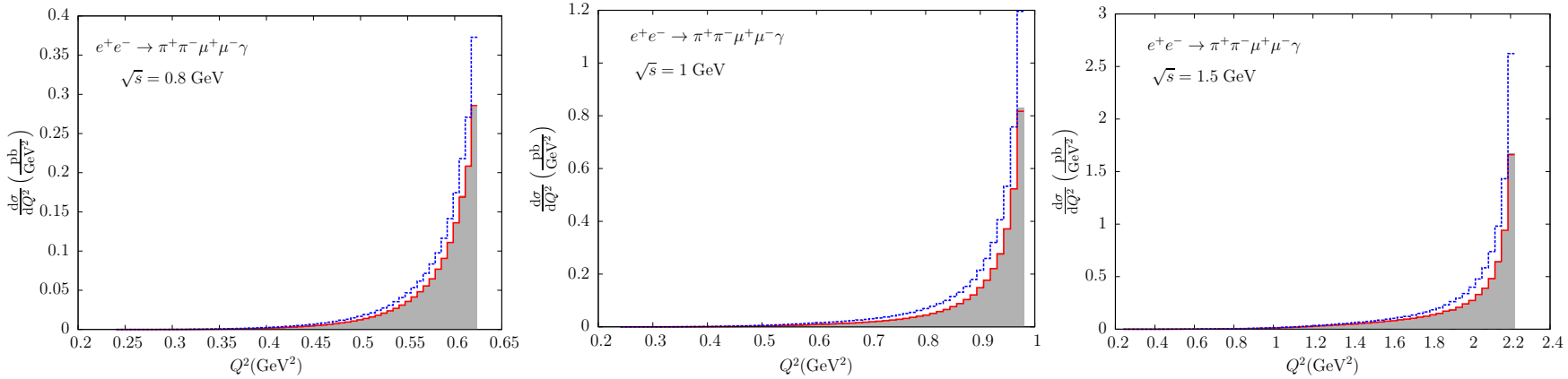

The differential cross sections of $e^+e^- \to \pi^+\pi^-\mu^+\mu^-\gamma$ as functions of invariant mass of the $\pi^+\pi^-\mu^+\mu^-$-system.

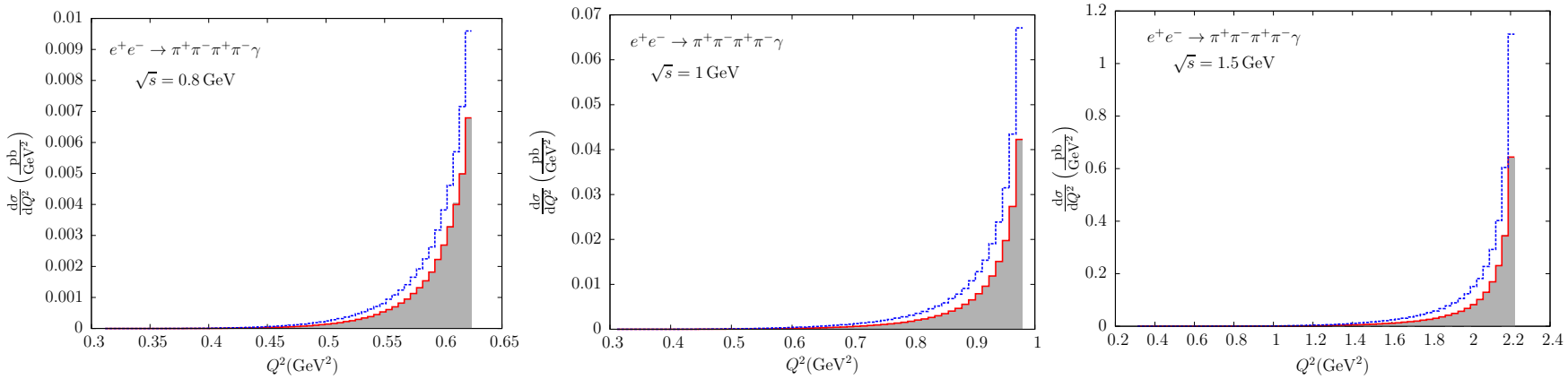

The differential cross sections of $e^+e^- \to \pi^+\pi^-\pi^+\pi^-\gamma$ as functions of invariant mass of the $\pi^+\pi^-\pi^+\pi^-$-system.

In following Fig, we make the same comparison for the cross sections of process $e^+e^- \to \pi^+\pi^-\mu^+\mu^-\gamma$ to be compared with previous $e^+e^- \to \pi^+\pi^-\gamma$ plot. This time `carlomat_3.1` generates 627 Feynman diagrams in the HLS model with the fixed couplings.

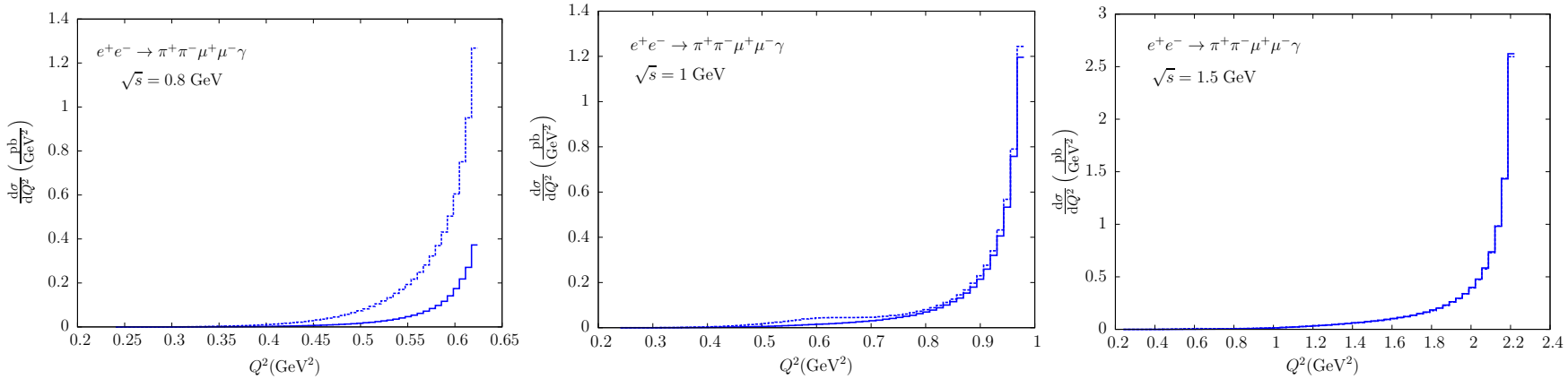

The differential cross sections of $e^+e^- \to \pi^+\pi^-\mu^+\mu^-\gamma$ as functions of invariant mass of the $\pi^+\pi^-\mu^+\mu^-$-system computed in a model with the charged pion form factor (solid lines) and in the HLS model with fixed couplings (dotted lines).

To illustrate the effect of the FSR in processes with two photons, the ISR (shaded histograms) and full LO (dashed lines) differential cross sections We see that this time the FSR effect is much bigger.

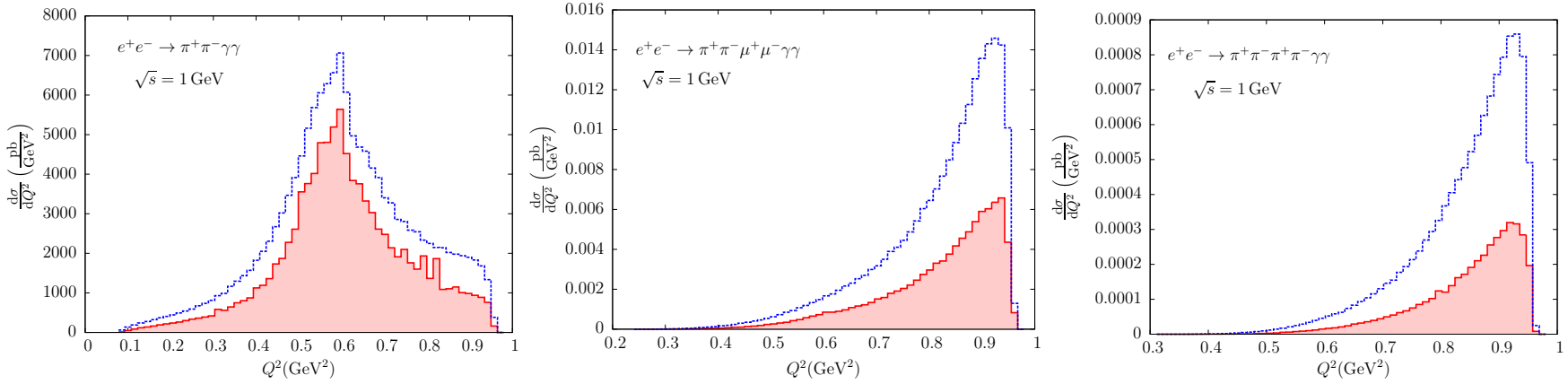

The differential cross sections of $e^+e^- \to \pi^+\pi^-\gamma\gamma$, $e^+e^- \to \pi^+\pi^-\mu^+\mu^-\gamma\gamma$ and $e^+e^- \to \pi^+\pi^-\pi^+\pi^-\gamma\gamma$ at $\sqrt{s} = 1$ GeV as functions of invariant mass of the $\pi^+\pi^-$-, $\pi^+\pi^-\mu^+\mu^-$ and $\pi^+\pi^-\pi^+\pi^-$-systems, respectively.

Conclusion

❒ we implemented $e^+e^- \to$ hadrons at low centre-of-mass energies in `carlomat_3.1` with pionform factor

❒ we have illustrated possible applications of the program by considering a photon radiation off the initial and final state particles for a few potentially interesting processes involving charged pion pairs.

❒ we have also discussed some problems related to the $U(1)$ electromagnetic gauge invariance that may arise if the momentum transfer dependence is introduced in the couplings of the HLS model or a set of the couplings implemented in the program is incomplete.

Thank you for your attention!